



This article appeared in

Sun, S., Tang, F., Imoto, S., Moberg, D. R., Ohto, T., Paesani, F., et al. (2018). Orientational Distribution of Free O-H Groups of Interfacial Water is Exponential. *Physical Review Letters*, 121(24): 246101. doi:10.1103/PhysRevLett.121.246101.

DOI: [10.1103/PhysRevLett.121.246101](https://doi.org/10.1103/PhysRevLett.121.246101)

Orientational Distribution of Free O-H Groups of Interfacial Water is Exponential

Shumei Sun, Fujie Tang, Sho Imoto, Daniel R. Moberg, Tatsuhiko Ohto, Francesco Paesani, Mischa Bonn, Ellen H. G. Backus, and Yuki Nagata

The Orientational Distribution of Free O-H Groups of Interfacial Water Is Exponential

Shumei Sun,^{1,#} Fujie Tang,^{1,2,#} Sho Imoto,¹ Daniel R. Moberg,³ Tatsuhiko Ohto,⁴ Francesco
Paesani,³ Mischa Bonn,^{1*} Ellen H. G. Backus,^{1*} and Yuki Nagata^{1*}

1. Max Planck Institute for Polymer Research, Ackermannweg 10, 55128 Mainz, Germany
2. International Center for Quantum Materials, Department of Physics, Peking University, 5 Yiheyuan Road, Haidian, Beijing 100871, China
3. Department of Chemistry and Biochemistry, University of California, San Diego, La Jolla, California 92093, United States
4. Graduate School of Engineering Science, Osaka University, 1-3 Machikaneyama, Toyonaka, Osaka 560-8531, Japan

These authors equally contributed to this work.

*Email: nagata@mpip-mainz.mpg.de, backus@mpip-mainz.mpg.de, bonn@mpip-mainz.mpg.de

Abstract

The orientational distribution of free O-H (O-D) groups at the H₂O (D₂O)-air interface is investigated using combined molecular dynamics (MD) simulations and sum-frequency generation (SFG) experiments. The average angle of the free O-H groups, relative to the surface normal, is found to be $\sim 63^\circ$, substantially larger than previous estimates of 30 - 40°. This discrepancy can be traced to erroneously assumed Gaussian/stepwise orientational distributions of free O-H groups. Instead, MD simulation and SFG measurement reveal a broad and exponentially decaying orientational distribution. The broad orientational distribution indicates the presence of the free O-H group pointing *down* to the bulk. We ascribe the origin of such free O-H groups to the presence of capillary waves on the water surface.

Main Text

1 At the interface of water with hydrophobic media, the hydrogen-bond (H-bond) network of
2 water is interrupted, making the O-H groups of the topmost interfacial water molecules
3 dangling (free) from the H-bond network. These free O-H groups are important for
4 determining the energetics of the water surface and are thereby critical for explaining the
5 exceptionally high surface tension of water. Furthermore, free O-H groups provide a unique
6 platform for hydrophobic hydration assembly [1–3], on-water catalysis [4], and growth of
7 aerosol particles [5,6]. As such, there have been many efforts to quantify the number and
8 orientation of free O-H groups at different aqueous interfaces.

9 The free O-H (O-D) groups of interfacial water can be studied experimentally by a sharp
10 peak at ~ 3700 (~ 2740) cm^{-1} in the surface-specific vibrational sum-frequency generation (SFG)
11 spectrum [7–12]. The frequency of the free O-H signal has been examined to determine the
12 interaction strength of the topmost water layer and the hydrophobic medium [13–17].
13 Moreover, the free O-H SFG response measured with different polarization combinations
14 provides information about their orientation. From the *ssp*-SFG (shorthand for *s*, *s*, and *p*
15 polarized sum-frequency output, visible input, and infrared input, respectively) and *ppp*-SFG
16 signals of the free O-H stretch, the averaged angle of the free O-H group at the water-air
17 interface has previously been estimated to $30\text{--}40^\circ$ [17–19]. The orientational distribution of
18 the free O-H group has been concluded to broaden with increasing temperature induced by
19 disordering of the topmost water layer [20,21]. However, to connect the *ppp*-/*ssp*-SFG peak
20 amplitudes of the free O-H stretch (A_{ppp} and A_{ssp} , respectively) with the averaged angle of the
21 free O-H group, one needs to assume a functional form for the orientational distribution of
22 the free O-H groups. So far, the distribution has been assumed to be stepwise
23 shaped [18,20,21] or Gaussian shaped [17,19].

1 Recently, we have developed a geometrical definition of the free O-H group [22] and,
2 based on this definition, we computed the orientation of the free O-H group from molecular
3 dynamics (MD) simulations with the POLI2VS model [23]. Surprisingly, these simulations
4 predict an average angle formed by the free O-H group and the surface normal to be $\sim 63^\circ$ [22],
5 much larger than the previously estimated values of $30\text{-}40^\circ$ [17–19]. This discrepancy casts
6 doubts on either the quality of the water force field model or the assumption of the
7 Gaussian/stepwise shaped orientational distribution of the free O-H groups.

8 Here, by combining simulation and experiment, we unveil the orientational
9 distribution of the free O-H group at the water-air interface. We compare the results of MD
10 simulations with various force field models, which commonly predict an average angle of ~ 63
11 $\pm 3^\circ$. Furthermore, these results suggest that the orientational distribution of the free O-H
12 group cannot be accurately represented by a narrow Gaussian or stepwise shaped distribution.
13 Rather, the distribution is exponentially shaped. The combination of a large average
14 orientation angle and an exponentially shaped distribution fully accounts for the experimental
15 data. We discuss the sensitivity of the free O-H SFG feature to the average angle and present
16 a physical argument for the existence of a broad orientational distribution.

17 We performed MD simulations of the water/air interface to characterize the structure
18 of the free O-H group for various force field models. To define the free O-H group, we used
19 the free O-H group definition developed recently in Ref. [22]. According to this definition, an
20 O-H group of water is free of hydrogen bonds when the intermolecular O...O distance is larger
21 than 3.5 \AA , and the H-O...O angle is larger than 50° . We used fixed-charge force field models
22 (TIP3P, [24] TIP4P, [24] TIP4/2005, [25] TIP4P/Ew [26], TIP4P/ice [27], SPC [28], SPC/E [29],
23 and SPC/Fw [30]), a polarizable model (POLI2VS [23]), and a many-body model (MB-pol [31–
24 33]). Simulation details can be found in Supplementary Materials.

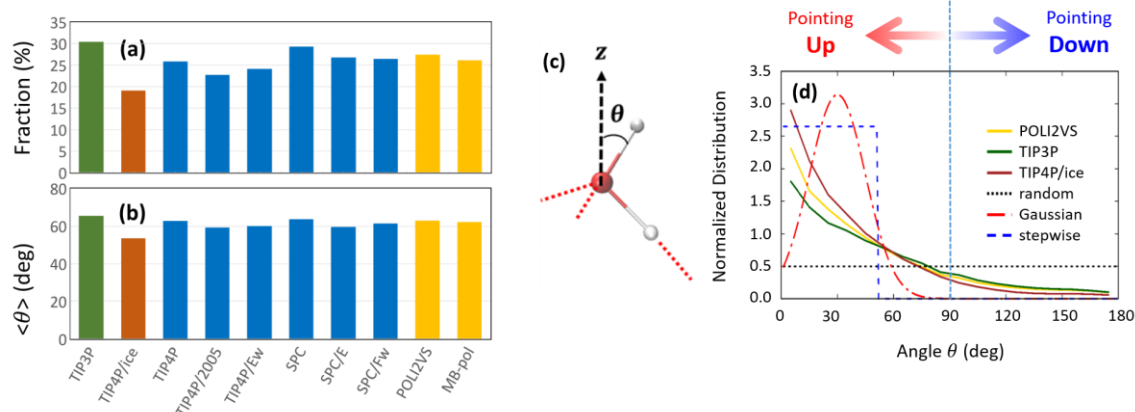


Figure 1. (a) Fractions of the water molecules with free O-H groups, and (b) average angles $\langle \theta \rangle$, computed from the MD simulations with various force field models. (c) Definition of the angle θ formed by the free O-H group and the macroscopic surface normal. (d) Normalized probability distributions of θ obtained from the POLI2VS, TIP3P and TIP4P/ice MD simulations as well as the stepwise function with $\theta_s = 51^\circ$ [18], and the Gaussian function with $\theta_G = 30^\circ$ and $\sigma = 15^\circ$ [19].

Figure 1(a) shows the simulated fraction of the interfacial water molecules with free O-H groups. The procedure for calculating the fraction of the free O-H groups is detailed in Supplementary Materials. The TIP4P/ice model provides the lowest fraction ($\sim 20\%$), while the TIP3P model provides the highest fraction ($\sim 30\%$). Since the TIP4P/ice model is parameterized to reproduce the properties of ice [27], it tends to overestimate the strengths of the H-bonds of water, decreasing the fraction of free O-H groups at the interface. In contrast, the TIP3P model is known to predict extremely short H-bond lifetime [30], indicating that the strength of the H-bonds in the TIP3P model is weaker than in the other water force field models. Thus, the TIP3P model predicts the highest fraction of the free O-H group. The fractions of the free

1 O-H group for various force field models are $25 \pm 5 \%$, which is consistent with experimental
2 data [34].

3 Figure 1(b) displays the average angle $\langle \theta \rangle$ formed by the free O-H groups and the
4 surface normal (see Figure 1(c)), where the thermal average of quantity A is calculated as
5 $\langle A \rangle = \int_0^\pi A f(\theta) \sin \theta d\theta$ and $f(\theta)$ is the orientational distribution of the free O-H groups.
6 Again, the TIP4P/ice and TIP3P models provide the lower and upper limits, respectively,
7 among all models considered in this study. $\langle \theta \rangle$ of the free O-H groups is $59 - 66^\circ$. This is,
8 however, in stark contrast with the previously reported values of 33.5° in Ref. [18] and 36.6°
9 in Ref. [19].

10 These values of 33.5° and 36.6° were obtained from a comparison of *ssp*- and *ppp*-SFG
11 intensity measurements in the following way. From the measured SFG intensity in *ssp* and *ppp*
12 polarizations (proportional to $|\chi_{ssp}^{(2),\text{eff}}|^2$ and $|\chi_{ppp}^{(2),\text{eff}}|^2$, respectively), $\chi_{xxz}^{(2)} = \chi_{yyz}^{(2)}$ and $\chi_{zzz}^{(2)}$
13 are obtained via:

$$14 \quad \chi_{ssp}^{(2),\text{eff}} = L_{yy}(\omega)L_{yy}(\omega_1)L_{zz}(\omega_2) \sin\beta_2 \chi_{yyz}^{(2)} \quad (1)$$

$$15 \quad \chi_{ppp}^{(2),\text{eff}} \approx -L_{xx}(\omega)L_{xx}(\omega_1)L_{zz}(\omega_2)\cos\beta\cos\beta_1\sin\beta_2\chi_{xxz}^{(2)} \\ 16 \quad +L_{zz}(\omega)L_{zz}(\omega_1)L_{zz}(\omega_2)\sin\beta\sin\beta_1\sin\beta_2\chi_{zzz}^{(2)} \quad (2)$$

17 where L_{ii} ($i = x, y, z$) is the Fresnel Factor and β_i is the incidence/reflection angle of the light
18 of frequency ω_i with respect to the surface normal. Here, the x-y plane is defined parallel to
19 the surface and the z-axis forms the macroscopic surface normal. The amplitudes of the free
20 O-H peak A_{xxz} and A_{zzz} in the $\chi_{xxz}^{(2)}$ and $\chi_{zzz}^{(2)}$ spectra, respectively, are related to $\langle \cos^3 \theta \rangle /$
21 $\langle \cos \theta \rangle$ via:

$$\frac{A_{xxz}}{A_{zzz}} \propto \frac{(1+r)\langle \cos\theta \rangle - (1-r)\langle \cos^3\theta \rangle}{2r\langle \cos\theta \rangle + 2(1-r)\langle \cos^3\theta \rangle} \quad (3)$$

in the slow motion limit [18], and is linked to $\langle \cos^2\theta \rangle$ via:

$$\frac{A_{xxz}}{A_{zzz}} \propto \frac{(1+r) - (1-r)\langle \cos^2\theta \rangle}{2r + 2(1-r)\langle \cos^2\theta \rangle} \quad (4)$$

in the fast motion limit [19]. For the slow (fast) motion limit, the decay of the orientational memory of the free O-H group is much slower (faster) than vibrational relaxation. r is given by the ratio of the transition polarizability $\alpha_{\zeta\zeta}/\alpha_{\xi\xi}$, where ξ and ζ denote the directions parallel to and perpendicular to the O-H bond, respectively (see Supplementary Materials). To obtain the average angle $\langle \theta \rangle$ from $\langle \cos^3\theta \rangle/\langle \cos\theta \rangle$ or $\langle \cos^2\theta \rangle$, one needs to assume an orientational distribution. Previously, a stepwise function [18,20,21]:

$$f(\theta) = \begin{cases} N_S & \text{for } 0 \leq \theta \leq \theta_S \\ 0 & \text{for } \theta_S < \theta < \pi \end{cases}, \quad (5)$$

and Gaussian function [17,19]:

$$f(\theta) = \frac{N_G}{\sqrt{2\pi\sigma^2}} e^{-(\theta-\theta_G)^2/2\sigma^2}, \quad (6)$$

have been used, where N_S and N_G are determined from the normalization condition;

$$\int_0^\pi f(\theta) \sin\theta d\theta = 1. \quad (7)$$

Since the discrepancy between $\langle \theta \rangle = 63^\circ$ in the simulation [22] and $\sim 35^\circ$ deduced from the experiments [18,19] may arise from the improperly assumed orientational distributions, we calculated the angular distributions from the MD simulations. These are displayed in Figure 1(d). The shapes of the computed distributions are very similar for different force field models,

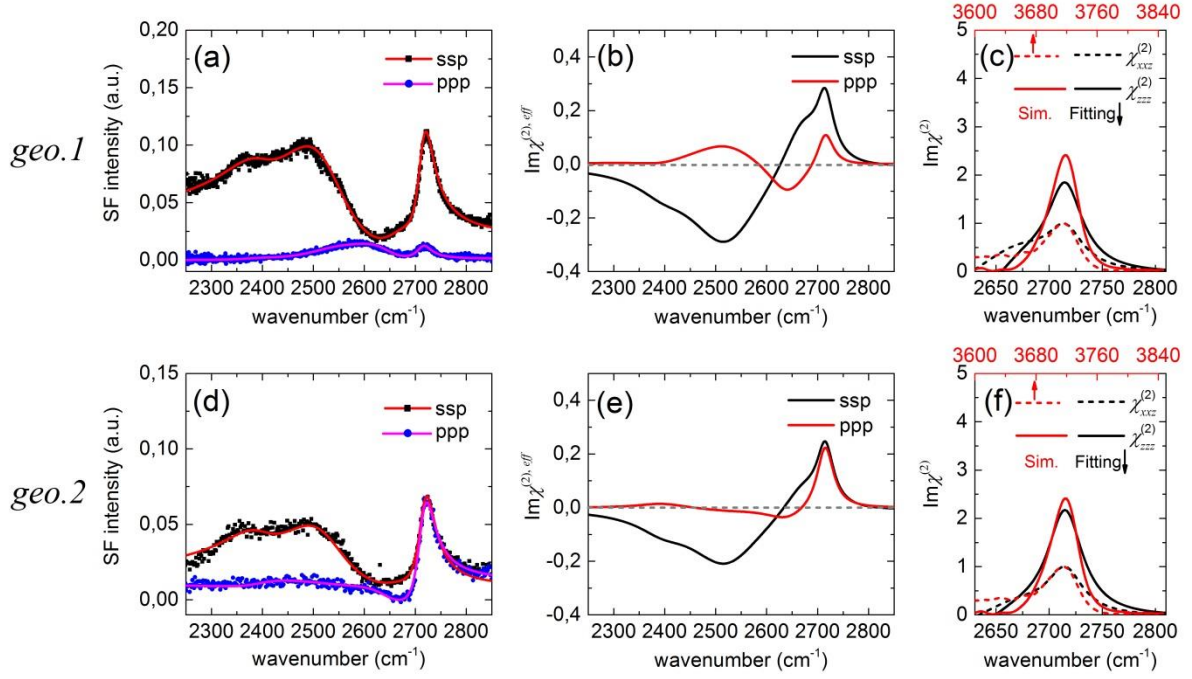
1 but differ significantly from the narrow Gaussian/stepwise shaped distributions. We find that
 2 the simulated distributions can be described well by an exponential curve:

$$3 \quad f(\theta) = N_E e^{-\theta/\theta_E}, \quad (8)$$

4 where N_E is the normalization parameter satisfying Eq. (7). For the POLI2VS model, $\theta_E = 53.3^\circ$.
 5 This illustrates that the Gaussian/stepwise shaped distributions are not appropriate for
 6 describing the free O-H group orientation at the water-air interface.

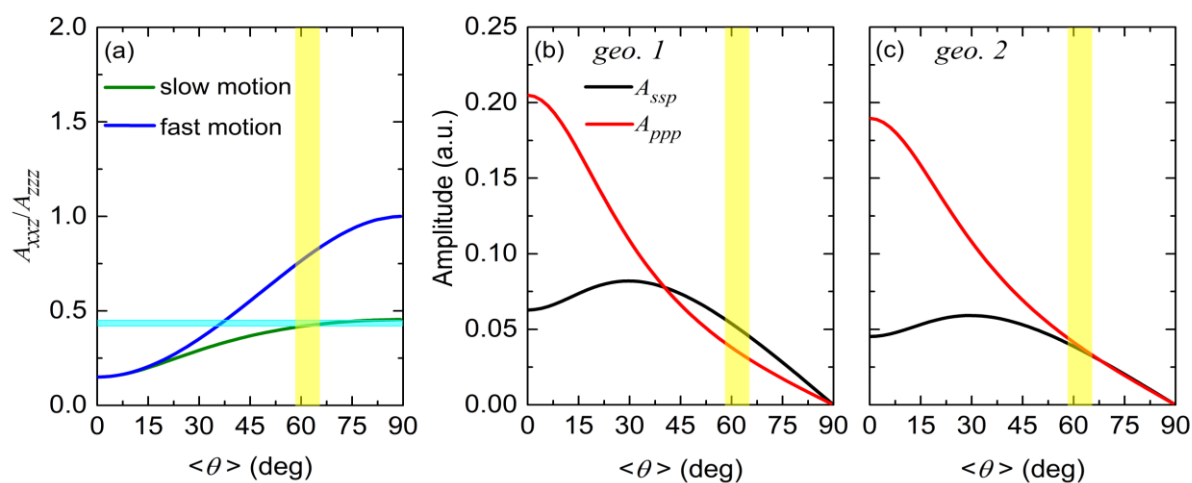
7 To examine whether this broad, exponentially decaying distribution of free O-H angles
 8 is consistent with the experimental data, we carried out SFG measurements with *ssp*- and *ppp*-
 9 polarization combinations at the D₂O-air interface. Since the *ppp*-SFG signal is sensitive to the
 10 experimental setup geometry, we used two experimental geometries to verify that the ratio
 11 of the amplitude for the free O-D group (A_{xxz}/A_{zzz}) is robust. In the experimental geometry
 12 1, the incident angles of IR and visible are 62° and 47° , respectively, while in geometry 2, the
 13 incident angles of IR and visible are 40° and 56° , respectively. The SFG intensity data are
 14 plotted in Figure 2(a) and (d), respectively. By fitting the intensity spectra (parameters are
 15 listed in Supplementary Materials), we obtained $\text{Im}(\chi_{ssp}^{(2),\text{eff}})$ and $\text{Im}(\chi_{ppp}^{(2),\text{eff}})$. These are
 16 plotted in Figure 2(b) and (e) for geometry 1 and 2, respectively. Furthermore, we obtained
 17 $\text{Im}(\chi_{xxz}^{(2)})$ and $\text{Im}(\chi_{zzz}^{(2)})$ from $\text{Im}(\chi_{ssp}^{(2),\text{eff}})$ and $\text{Im}(\chi_{ppp}^{(2),\text{eff}})$ via Eqs. (1) and (2), where the
 18 calculation of Fresnel factors is detailed in Supplementary Materials. These are displayed in
 19 Figure 2(c) and (f) for geometry 1 and 2, respectively. $\text{Im}(\chi_{xxz}^{(2)})$ and $\text{Im}(\chi_{zzz}^{(2)})$ spectra show
 20 that the two data sets of the different incident angles are in good agreement. From these
 21 spectra, we obtain a ratio of A_{xxz}/A_{zzz} of 0.43 ± 0.02 (geometry 1: 0.45, geometry 2: 0.42,
 22 see Sec. III. C of Supplementary Materials). Furthermore, as is seen in Figure 2(c) and (f), the

1 simulated $\text{Im}(\chi_{xxz}^{(2)})$ and $\text{Im}(\chi_{zzz}^{(2)})$ data with the POLI2VS model [23] are also in good
 2 agreement with the experimental data.



3
 4
 5 Figure 2. (a) *ssp*- and *ppp*-SFG intensity spectra of D₂O at the D₂O-air interface, (b) imaginary
 6 part of the effective spectra containing the Fresnel factors; $\text{Im}(\chi_{ssp}^{(2),\text{eff}})$ and $\text{Im}(\chi_{ppp}^{(2),\text{eff}})$
 7 obtained from the fit of the intensity spectra, (c) $\text{Im}(\chi_{xxz}^{(2)})$ and $\text{Im}(\chi_{zzz}^{(2)})$ constructed from
 8 $\text{Im}(\chi_{ssp}^{(2),\text{eff}})$ and $\text{Im}(\chi_{ppp}^{(2),\text{eff}})$ for experimental geometry 1, and (d) *ssp*- and *ppp*-SFG intensity
 9 spectra (e) $\text{Im}(\chi_{ssp}^{(2),\text{eff}})$ and $\text{Im}(\chi_{ppp}^{(2),\text{eff}})$, (f) $\text{Im}(\chi_{xxz}^{(2)})$ and $\text{Im}(\chi_{zzz}^{(2)})$ for experimental
 10 geometry 2. In (a) and (d), the fit data is also shown. In (c) and (f), simulated data for H₂O with
 11 the POLI2VS model is also shown. $\text{Im}(\chi_{xxz}^{(2)})$ and $\text{Im}(\chi_{zzz}^{(2)})$ in (c) and (f) were normalized,
 12 based on the free O-D peak amplitude in $\text{Im}(\chi_{xxz}^{(2)})$.

1 The experimentally obtained $A_{xxz}/A_{zzz} = 0.43 \pm 0.02$ can now be compared with the
 2 simulation data. To do so, we calculated the variation of A_{xxz}/A_{zzz} as a function of $\langle\theta\rangle$ for the
 3 exponential shaped distribution (Eq. (8)), by using Eqs. (3) and (4) with $r = 0.15$. Although this
 4 r was set to 0.32 in Ref. [35], we used $r = 0.15$ obtained from *ab initio* calculation of water
 5 trimer at the B3LYP/aug-cc-pVTZ level of theory (see Supplementary Materials). The data is
 6 shown in Figure 3(a). $\langle\theta\rangle = 63 \pm 3^\circ$ provides the A_{xxz}/A_{zzz} value of 0.42 ± 0.01 for the slow
 7 motion limit and 0.80 ± 0.04 for the fast motion limit. The value of 0.42 for the slow motion
 8 limit together with the exponential shaped distribution is consistent with the experimental
 9 result of 0.43 ± 0.02 , manifesting that a broad exponentially shaped distribution and the
 10 expression of the slow motion limit (Eq. (8)) can indeed account for the experimental data.

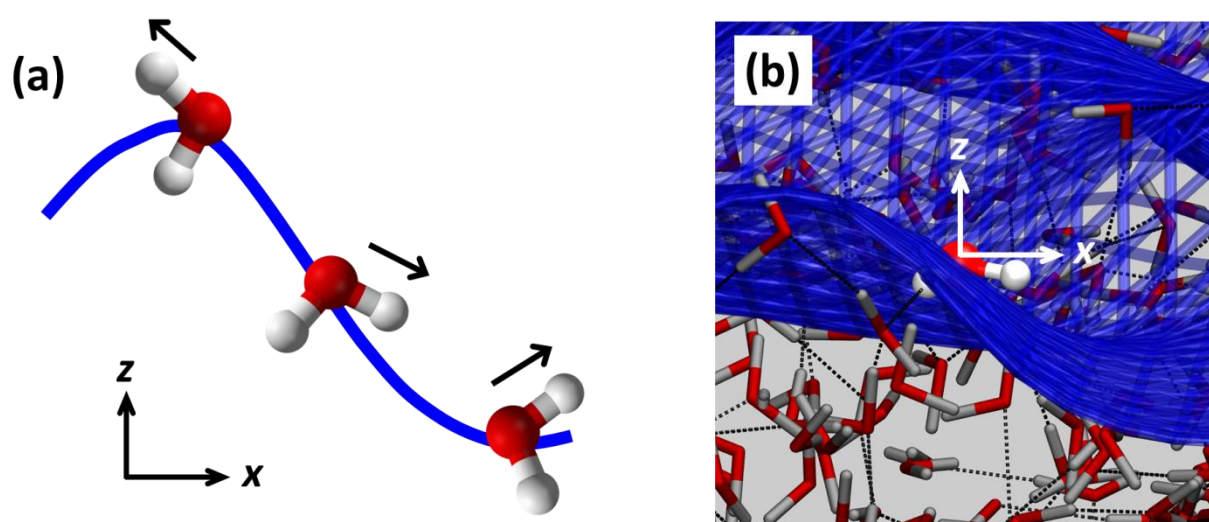


11
 12 Figure 3. (a) Variations of A_{xxz}/A_{zzz} as a function of average angle $\langle\theta\rangle$ computed based on
 13 the exponential distribution represented by Eq. (8). The sky blue zone represents the
 14 experiment tolerance and the yellow zone represents the simulation tolerance. A_{ssp} and A_{ppp}
 15 vs. $\langle\theta\rangle$ based on the slow motion approximation and exponential shaped orientational
 16 distribution for (b) experimental setup geometry 1 and (c) geometry 2.

1 The broad exponentially shaped distribution has two important consequences. One is
2 that both the *ssp*- and *ppp*-SFG amplitudes of the free O-H (O-D) stretch (A_{ssp} and A_{ppp} ,
3 respectively) are very sensitive to the average angle of the free O-H group around 63° as is
4 seen in Figure 3(b) and (c). This observation contrasts the previous conclusion that *ssp*-signals
5 would be insensitive to the angle of the free O-H group [18,20,21]. Our finding indicates that
6 the variation of A_{ssp} cannot be solely attributed to the variation of the number of free O-H
7 (O-D) stretch chromophores when the average angle is larger than 50° . This can resolve the
8 apparent contradiction on the surface activity of small osmolyte molecules at the water-air
9 interface: the absence of the osmolyte in the topmost water layer has been concluded from
10 the insensitivity of the free O-H stretch *ssp*-SFG peak to the addition of osmolyte [36,37], while
11 MD simulations have suggested that osmolyte molecules should be located at the topmost
12 water layer [38,39]. Since the average angle of the free O-H group changes due to the addition
13 of osmolyte, the reduction of the free O-H stretch chromophores is compensated by the
14 decrease in $\langle\theta\rangle$ (increase in $\langle\cos\theta\rangle$), yielding no overall change in the SFG peak amplitude [40].
15 Hence, the SFG intensity remains constant due to a cancellation of counteracting effects. **The**
16 **appearance of TMAO at the topmost water layer demonstrates that the methyl group of**
17 **TMAO is very hydrophobic, which is critical to account for the counteracting effects of TMAO**
18 **and urea on the protein folding. [41,42] Furthermore, this work suggests that** the orientational
19 distribution should be carefully examined to obtain the average angles not only for the O-H
20 stretch mode of water but also for the C=O, N-H and C-H stretch mode. These modes have
21 been frequently used for probing proteins [43,44], a small molecule [45], and lipids [46,47] at
22 the water-air interface as well as the ionic liquid-air interface [48–51].

23 The other consequence is that for the broad exponential distribution with $\theta_E = 53.3^\circ$
24 in Eq. (8), ~20 % of the free O-H groups at the water-air interface point *down* to the bulk,

1 unlike the narrow Gaussian/stepwise shaped distributions. In fact, a free O-H group pointing
2 down has not been recognized [52]. The mechanism of the presence of free O-H group
3 pointing down can be understood by considering capillary waves causing surface roughness.
4 On the top and bottom of the capillary wave, *i.e.*, the location where the gradient of the
5 capillary wave is small, a free O-H group rarely points *down* to the bulk. In contrast, on the
6 slope of the capillary wave, *i.e.*, the location where the gradient is very large, a free O-H group
7 often points *down* to the bulk. This is schematically shown in Figure 4(a). A water molecule
8 with a free O-H group pointing *down* to the bulk can be often found on the slope of the
9 capillary wave, as apparent from the simulation snapshot shown in Figure 4(b). When we
10 remove the surface roughness by using the instantaneous liquid interface, the free O-H group
11 orientation distribution becomes substantially narrower (see Figure S5). This clearly
12 demonstrates that interfacial molecular orientation is strongly affected by capillary waves.



14
15 Figure 4 (a) Schematic of the interfacial water molecules. The blue line represents the capillary
16 wave, and the black arrows denote the orientation of the free O-H group. (b) Snapshot of the
17 simulated water-air interface. A water molecule with the free O-H group is highlighted with

1 spheres for atoms. The black broken lines represent the hydrogen bonds, and the blue lines
2 represent the positions of the capillary wave.

3
4 In conclusion, by combining SFG experiment and MD simulations, we examined the
5 orientational distribution of the free O-H group at the water-air interface. The different force
6 field models provide the average angle of the free O-H group of $\sim 63^\circ$, substantially larger than
7 previous estimates of $30\text{--}40^\circ$ [17–19]. The underestimation of the angle for the previous
8 studies arises from the assumed shape of the orientational distributions; the actual
9 distribution of the free O-H orientation is much broader and exponentially shaped. This leads
10 to a high sensitivity of the SFG amplitude of the free O-H stretch mode at the *ssp* polarization
11 combination to the angle of the free O-H group, opposed to the commonly claimed
12 insensitivity of the *ssp*-SFG signal to the angle. Furthermore, a broad distribution indicates
13 that $\sim 20\%$ of the free O-H groups point down to the bulk. We attribute this to the free O-H
14 groups on the slope of a capillary wave.

16 **Acknowledgment**

17 This work was partly funded by an ERC Starting Grant (Grant No. 336679) and a DFG
18 grant (no. BA 5008/3). D.R.M. and F.P. were supported by the National Science Foundation
19 (Grant. No. CHE-1453204) and used computational resources of the Extreme Science and
20 Engineering Discovery Environment (XSEDE), which is supported by the National Science
21 Foundation (Grant No. ACI-1053575).

1 **References:**

- 2 [1] Y. Jung and R. A. Marcus, *J. Am. Chem. Soc.* **129**, 5492 (2007).
- 3 [2] D. Chandler, *Nature* **437**, 640 (2005).
- 4 [3] S. Narayan, J. Muldoon, M. G. Finn, V. V. Fokin, H. C. Kolb, and K. B. Sharpless, *Angew.*
5 *Chemie - Int. Ed.* **44**, 3275 (2005).
- 6 [4] B. Braunschweig, S. Eissner, and W. Daum, *J. Phys. Chem. C* **3**, 1751 (2008).
- 7 [5] J. Julin, M. Shiraiwa, R. E. H. Miles, J. P. Reid, U. Pöschl, and I. Riipinen, *J. Phys. Chem.*
8 *A* **117**, 410 (2013).
- 9 [6] J. F. Davies, R. E. H. Miles, A. E. Haddrell, and J. P. Reid, *Proc. Natl. Acad. Sci. U. S. A.*
10 **110**, 8807 (2013).
- 11 [7] J. A. McGuire and Y. R. Shen, *Science* **313**, 1945 (2006).
- 12 [8] I. V. Stiopkin, C. Weeraman, P. A. Pieniazek, F. Y. Shalhout, J. L. Skinner, and A. V.
13 Benderskii, *Nature* **474**, 192 (2011).
- 14 [9] A. M. Jubb, W. Hua, and H. C. Allen, *Annu. Rev. Phys. Chem.* **63**, 107 (2012).
- 15 [10] C.-S. Tian and Y. R. Shen, *J. Am. Chem. Soc.* **131**, 2790 (2009).
- 16 [11] S. Nihonyanagi, S. Yamaguchi, and T. Tahara, *J. Chem. Phys.* **130**, 204704 (2009).
- 17 [12] S. Yamaguchi, *J. Chem. Phys.* **143**, 034202 (2015).
- 18 [13] L. F. Scatena, M. G. Brown, and G. L. Richmond, *Science*. **292**, 908 (2001).
- 19 [14] F. G. Moore and G. L. Richmond, *Acc. Chem. Res.* **41**, 739 (2008).

- 1 [15] C. S. Tian and Y. R. Shen, Proc. Natl. Acad. Sci. U. S. A. **106**, 15148 (2009).
- 2 [16] R. Vaécha, S. W. Rick, P. Jungwirth, A. G. F. De Beer, H. B. De Aguiar, J. S. Samson, and
3 S. Roke, J. Am. Chem. Soc. **133**, 10204 (2011).
- 4 [17] R.-R. Feng, Y. Guo, and H.-F. Wang, J. Chem. Phys. **141**, 18C507 (2014).
- 5 [18] X. Wei and Y. R. Shen, Phys. Rev. Lett. **86**, 4799 (2001).
- 6 [19] W. Gan, D. Wu, Z. Zhang, R. R. Feng, and H. F. Wang, J. Chem. Phys. **124**, 114705
7 (2006).
- 8 [20] X. Wei, P. B. Miranda, and Y. R. Shen, Phys. Rev. Lett. **86**, 1554 (2001).
- 9 [21] X. Wei, P. Miranda, C. Zhang, and Y. Shen, Phys. Rev. B **66**, 085401 (2002).
- 10 [22] F. Tang, T. Ohto, T. Hasegawa, W. J. Xie, L. Xu, M. Bonn, and Y. Nagata, J. Chem.
11 Theory Comput. **14**, 357 (2018).
- 12 [23] T. Hasegawa and Y. Tanimura, J. Phys. Chem. B **115**, 5545 (2011).
- 13 [24] W. L. Jorgensen, J. Chandrasekhar, J. D. Madura, R. W. Impey, and M. L. Klein, J. Chem.
14 Phys. **79**, 926 (1983).
- 15 [25] J. L. F. Abascal and C. Vega, J. Chem. Phys. **123**, 234505 (2005).
- 16 [26] H. W. Horn, W. C. Swope, J. W. Pitera, J. D. Madura, T. J. Dick, G. L. Hura, and T. Head-
17 Gordon, J. Chem. Phys. **120**, 9665 (2004).
- 18 [27] J. L. F. Abascal, E. Sanz, R. García Fernández, and C. Vega, J. Chem. Phys. **122**, 234511
19 (2005).
- 20 [28] H. J. C. Berendsen, J. P. M. Postma, W. F. van Gunsteren, and J. Hermans, *In*

1 *Intermolecular Forces: Proceedings of the Fourteenth Jerusalem Sympo- Sium on*
2 *Quantum Chemistry and Biochemistry Held in Jerusalem, Israel, April 13–16, 1981,*
3 *Edited by B. Pullman (1981).*

- 4 [29] H. J. C. Berendsen, J. R. Grigera, and T. P. Straatsma, *J. Phys. Chem.* **91**, 6269 (1987).
- 5 [30] Y. Wu, H. L. Tepper, and G. A. Voth, *J. Chem. Phys.* **124**, 024503 (2006).
- 6 [31] V. Babin, C. Leforestier, and F. Paesani, *J. Chem. Theory Comput.* **9**, 5395 (2013).
- 7 [32] V. Babin, G. R. Medders, and F. Paesani, *J. Chem. Theory Comput.* **10**, 1599 (2014).
- 8 [33] G. R. Medders, V. Babin, and F. Paesani, *J. Chem. Theory Comput.* **10**, 2906 (2014).
- 9 [34] Q. Du, E. Freysz, and Y. R. Shen, *Science* **264**, 826 (1994).
- 10 [35] Q. Du, R. Superfine, E. Freysz, and Y. R. Shen, *Phys. Rev. Lett.* **70**, 2313 (1993).
- 11 [36] M. Ahmed, V. Namboodiri, P. Mathi, A. K. Singh, and J. A. Mondal, *J. Phys. Chem. C*
12 **120**, 10252 (2016).
- 13 [37] J. A. Mondal, *J. Phys. Chem. Lett.* **7**, 1704 (2016).
- 14 [38] A. Fiore, V. Venkateshwaran, and S. Garde, *Langmuir* **29**, 8017 (2013).
- 15 [39] T. Ohto, J. Hunger, E. Backus, W. Mizukami, M. Bonn, and Y. Nagata, *Phys. Chem.*
16 *Chem. Phys.* **19**, 6909 (2017).
- 17 [40] T. Ohto, E. H. G. Backus, W. Mizukami, J. Hunger, M. Bonn, and Y. Nagata, *J. Phys.*
18 *Chem. C* **120**, 17435 (2016).
- 19 [41] S. Paul and G. N. Patey, *J. Am. Chem. Soc.* **129**, 4476 (2007).

- 1 [42] W. J. Xie, S. Cha, T. Ohto, W. Mizukami, Y. Mao, M. Wagner, M. Bonn, J. Hunger, and
2 Y. Nagata, *Chem* **4**, 1 (2018).
- 3 [43] J. Wang, S. H. Lee, and Z. Chen, *J. Phys. Chem. B* **112**, 2281 (2008).
- 4 [44] S. Ham, J. H. Kim, H. Lee, and M. Cho, *J. Chem. Phys.* **118**, 3491 (2003).
- 5 [45] D. Simonelli and M. J. Shultz, *J. Chem. Phys.* **112**, 6804 (2000).
- 6 [46] N. Takeshita, M. Okuno, and T. A. Ishibashi, *Phys. Chem. Chem. Phys.* **19**, 2060 (2017).
- 7 [47] G. Ma and H. C. Allen, *Langmuir* **22**, 5341 (2006).
- 8 [48] C. Peñalber-Johnstone, G. Adamová, N. V. Plechkova, M. Bahrami, T. Ghaed-Sharaf, M.
9 H. Ghatee, K. R. Seddon, and S. Baldelli, *J. Chem. Phys.* **148**, 193841 (2018).
- 10 [49] C. Aliaga and S. Baldelli, *J. Phys. Chem. B* **111**, 9733 (2007).
- 11 [50] T. Iwahashi, T. Miyamae, K. Kanai, K. Seki, D. Kim, and Y. Ouchi, *J. Phys. Chem. B* **112**,
12 11936 (2008).
- 13 [51] Y. Jeon, J. Sung, W. Bu, D. Vaknin, Y. Ouchi, and D. Kim, *J. Phys. Chem. C* **112**, 19649
14 (2008).
- 15 [52] J. N. Israelachvili, *Intermolecular and Surface Forces* (Academic press, 2011).
- 16
17
18
19